

Improving the triaxial bulge model of M31

Simon Berman¹ and Laurent Loinard²

¹ *Theoretical Physics, University of Oxford, 1 Keble Road, Oxford, UK; simon@thphys.ox.ac.uk*

² *Instituto de Astronomía, Universidad Nacional Autónoma de México, Apartado Postal 72–3, 58089 Morelia, Michoacán, México*

Accepted . Received ; in original form

ABSTRACT

A detailed hydrodynamical model of the gas flow in the triaxial gravitational potential of the bulge of the Andromeda galaxy (M31) has recently been proposed by Berman (2001), and shown to provide excellent agreement with the CO emission line velocities observed along its major axis. In the present paper, we confirm the validity of that model by showing that it can also reproduce the CO velocities observed off the major axis – a much more robust test. The CO observations, however, tend to span a wider range of velocities than a direct application of the original model of Berman would suggest. This situation can be improved significantly if the molecular disk is made thicker, a requirement already encountered in dynamical simulations of other spiral galaxies, and typically attributed to a broadening of the molecular layer in galactic fountain-like processes. In the central regions of M31, however, it is unclear whether there actually is a thick molecular disk, or whether broadening the molecular layer is merely an artificial theoretical means of accounting for some disk warping. Other effects not included in the model, such as hydraulic jumps, might also contribute to a widening of the velocities.

Key words: hydrodynamics – galaxies: M31 – galaxies: ISM – galaxies: structure – galaxies: evolution.

1 INTRODUCTION

There is growing evidence that spiral galaxies in which no bar is easily seen on optical or infrared images, nonetheless, have triaxial bulges. Twisting of the inner isophotes and misalignments between the disk and the bulge major axes (both of which have been detected in several spirals with no obvious bar) are clear signposts of triaxiality. Even stronger cases have been made by combining optical or infrared photometric data with spectroscopic observations of the gaseous interstellar component. Indeed, when submitted to a triaxial gravitational potential, the interstellar gas near the centre of a spiral galaxy can be found at higher velocities than expected from circular motion. Such anomalous velocities have been reported in several galaxies where no strong bar is visible, including the two nearest examples: the Milky Way (Rougoor & Oort 1959; Dame et al. 2001) and the Andromeda galaxy (Lindblad 1956; Loinard et al. 1999).

The triaxiality of spiral galaxy bulges is particularly important for two reasons. First, it can affect the dynamics of interstellar gas, gathering large amounts of it near galactic centres. This could help to explain the appearance of active galactic nuclei. On long timescales, a build of gas in galactic centres could affect the morphology of spiral galaxies, and imply secular changes in their Hubble types. Second, triax-

iality allows more constraints to be derived from spectral observations. In an axisymmetric system, the rotation curve only allows the determination of the radial mass distribution, without providing any three dimensional information. In particular, it is not possible to assess in an axisymmetric system whether the dark matter component is distributed in a flat disk-like structure or in a spherical halo. In a triaxial system, that disk–halo degeneracy can be removed, with obviously important consequences for our understanding of dark matter. Cold Dark Matter (CDM) models, for instance, favor spherical halos.

Since triaxiality primarily affects the dynamics at the centres of spiral galaxies, it should be sought in our neighbours, where the achievable linear resolution is highest. This is particularly important when using radio observations of the gaseous component, which often have limited angular resolutions. Detailed studies of the dynamics of the central regions of the Milky Way are adversely affected by our location inside of the system, and the well-known associated confusion and distance ambiguity problems. However, the existence of triaxial features in the inner Galaxy have been postulated for over forty years. Based on the discovery of the 3 kpc arm, Kerr (1967) proposed the existence of a gaseous bar at the Galaxy centre, and Mulder & Liem (1986) modelled the arm as a density wave in a barred potential. By combining photometric and kinematic data, Gerhard &

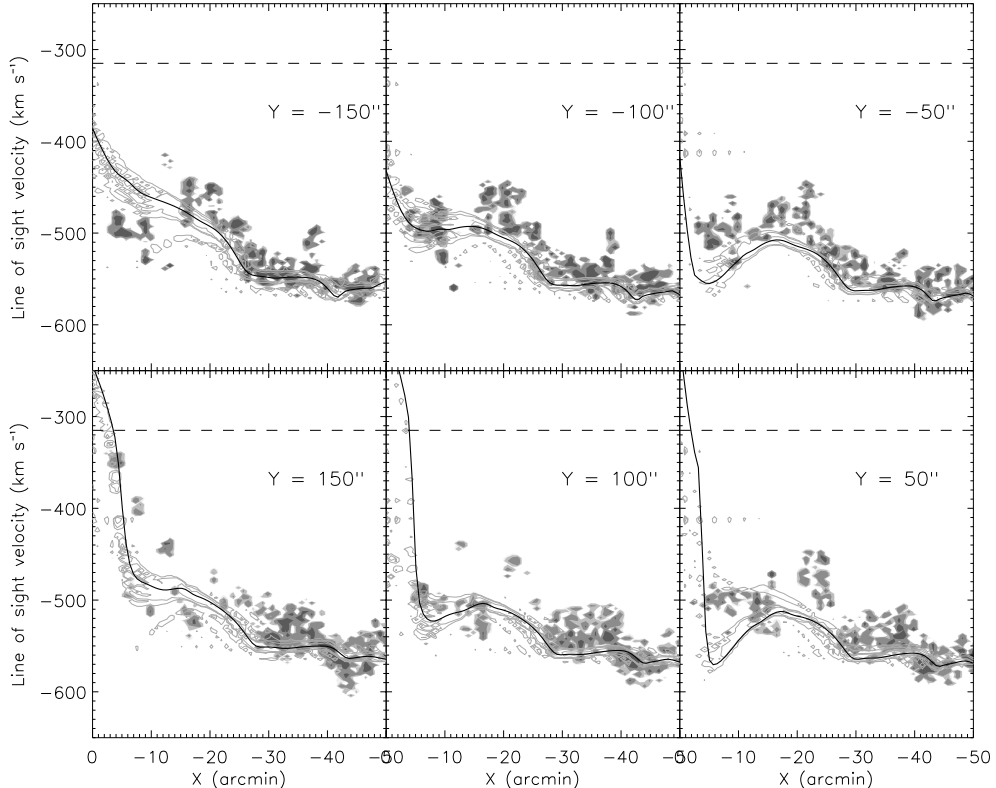


Figure 1. Comparison of CO observations and gas velocities from the model of maximum likelihood of Berman (2001) away from the line of nodes of the disk. Model data were convolved with the 2D function representing the FCRAO beam as described in the text. Intensity is plotted as a greyscale for observations and using contour levels for model data. Contours are given at 1, 3, 10 and 30% of the maximum value in each subplot. The dashed line indicates the systemic velocity and the solid line the results at Y arcsec ignoring the effects of the thick disk and of the beam function.

Vietri (1986) demonstrated the triaxiality of the Galactic bulge, and COBE images of the Galactic centre have confirmed this triaxiality (Dwek et al. 1995; Binney et al. 1997).

The next nearest spiral (the Andromeda Galaxy – M31) has no clear visible bar, and is an excellent target for a dynamics study, because its high inclination enables an accurate determination of the gas kinematics. M31 has long been known to have twisted inner isophotes and misaligned bulge and disk major axes (Lindblad 1956). Moreover, the existence of anomalous gas velocities in the inner few kiloparsecs is also now well established both for the atomic (Brinks & Burton 1984) and molecular (Loinard et al. 1996, 1999) components. A convincing interpretation in terms of triaxiality was put forward as early as 1956 by Lindblad, and was further developed by Stark (1977) and Stark & Binney (1994). However, those early works were hampered by the lack of strong observational constraints.

The distribution and kinematics of the atomic component of the interstellar medium (ISM) has long been known at high resolution and sensitivity across the entire disk of M31 thanks to interferometric observations of the 21-cm line of atomic hydrogen (Brinks & Shane 1984, and references therein). However, those observations do not provide clear information on the ISM kinematics in central regions, because the kinematic component associated with the warped outer disk can be seen in projection through the inner disk. The resulting confusion between inner and outer disk seen

in the H I position-velocity diagrams of the central regions of M31 precludes accurate studies of its dynamics. The molecular component traced by CO emission is a better tracer of the dynamics of the inner regions because no CO emission can be detected in the warped outer disk. However, the inner regions of M31 are also particularly dim in CO (Dame et al. 1993, Loinard et al. 1999). Fragmentary CO observations of the central regions of M31 were used to constrain the model of Stark & Binney (1994). Recently, however, more systematic CO observations have been obtained.

Loinard et al. (1995) presented a deep search for CO emission along the inner major axis of M31. This search confirmed the existence of anomalous velocities in the inner few kiloparsecs of M31, and results along the line of nodes of the disk were used by Berman (2001) to constrain an improved dynamical model of the central regions of M31 (see §2 below). However, Berman (2001) pointed out that off-axis CO observations would provide better constraints. Such data are now available – at least for the southern half of M31 – thanks to the CO(1-0) survey made at the *Five College Radio Astronomy Observatory* (FCRAO – Loinard et al. 1996, 1999). The angular resolution of the survey is ~ 1 arcmin, and it covers the entire Southern part of M31 with a sampling of 50 arcsec. The observational noise level is rather constant across the entire surveyed region with a typical r.m.s. of 45–50 mK per 3.25 km s^{-1} spectral channel. Although the CO(1-0) is found to peak in the broad Population I ring at

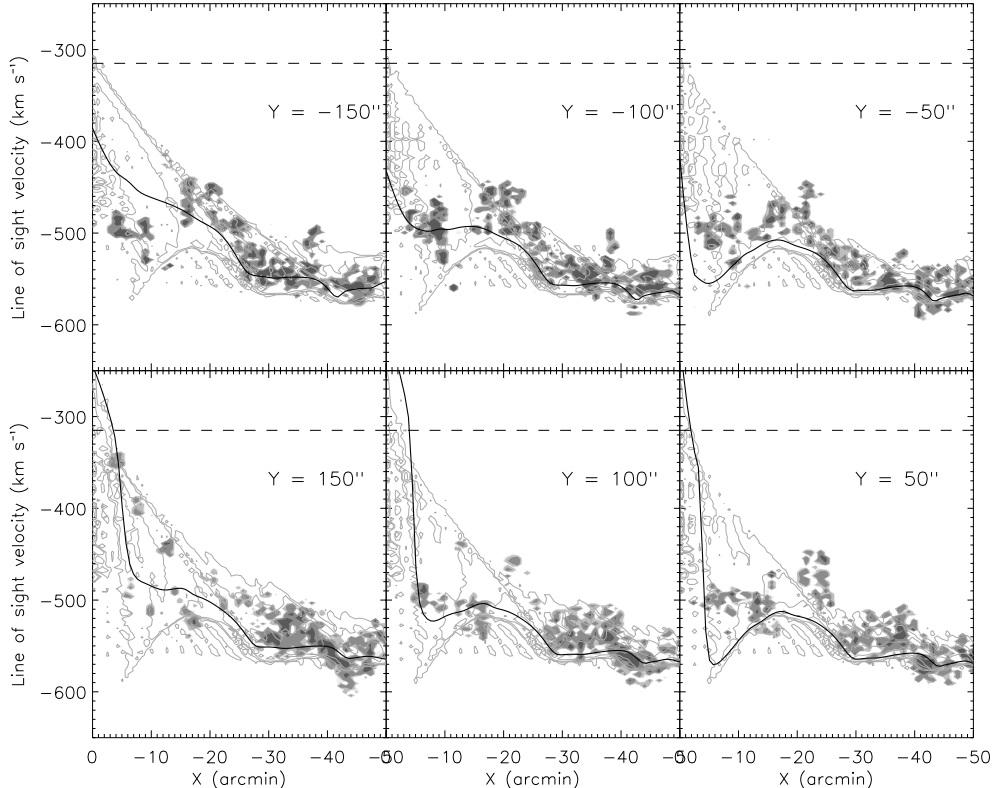


Figure 2. Comparison of CO observations and gas velocities from the model of maximum likelihood away from the line of nodes of the disk. The model includes a corotating thick disk of scale height $z_0 = 400$ pc. Model data were convolved with the 2D function representing the FCRAO beam as described in the text. Intensity is plotted as a greyscale for observations and using contour levels for model data. Contours are given at 1, 3, 10 and 30% of the maximum value in each subplot. The dashed line indicates the systemic velocity and the solid line the results at Y arcsec ignoring the effects of the thick disk and of the beam function.

10 kpc from the centre, significant emission is still detected in the inner 2–3 kpc (10–15 arcmin), where most constraints can be obtained about the triaxiality of the bulge. The integrated intensity images or position–velocity diagrams shown in Loinard et al. (1999), as well as the position–velocity diagrams that will be shown in this article, have been obtained after ‘unsharp masking’ was applied to the data. In this scheme, a data cube smoothed both in position and velocity (but not regridded) is first constructed from the original data. The average noise level σ in this smoothed cube is computed, and all the pixels in the non-smoothed data cube where no significant ($> 3\sigma$) emission is found in the smoothed version are blanked. This avoids that unnecessary noise is added when summations over several pixels are performed, and in effect reduces the noise in integrated maps by a factor of a few. A slight drawback of this method is that the noise becomes dependent on the number of pixels summed (or averaged), and, therefore, on the position in the maps.

Anomalous velocities are clearly seen in this data set in the inner regions of M31 (see fig. 12 in Loinard et al. 1999). While the cut along the major axis essentially shows the same anomalous velocities as reported by Loinard et al. (1995), cuts parallel to the major axis provide new constraints for the models, as called for by Berman (2001).

2 ORIGINAL MODEL

The dynamical model developed by Berman (2001) takes into account a rotating, triaxial bulge, and an axisymmetric component that mimics the combined influence of the disk and halo. The properties of the bulge are obtained by finding a triaxial mass distribution which gives the observed $R^{1/4}$ B -band surface brightness profile when rotated and inclined to the plane of the sky. Properties of the axisymmetric component are deduced from a simple interpretation of $\mathrm{H}\alpha$ and CO kinematics. The gas response to the gravitational potential is computed using a hydrodynamical code (GALAHAD) that solves the non-self gravitating, isothermal Euler equations, on a regular Cartesian grid, using the FS2 algorithm of van Albada et al. (1982). Each grid cell is 125 pc (37.5 arcsec) on a side, which is similar to the resolution (~ 60 arcsec) of the CO data. Removal and injection of interstellar matter by star-formation and stellar mass-loss respectively are included (somewhat crudely) in the algorithm.

Berman (2001) constrained the parameters of his model by comparing the output gas flow to the CO observations along the line of nodes of the disk of M31 of Loinard et al. (1995). The best fit to the data is obtained for a bulge semi-major axis $a = 3.5$ kpc, a pattern speed $\Omega_p = 53.7 \text{ km s}^{-1} \text{ kpc}^{-1}$, a corotation radius to bulge semi-major axis ratio $\mathcal{R} = 1.2$, an angle ϕ between the major axis of the bulge and the disk’s line of nodes of 15° , and a bulge mass-to-

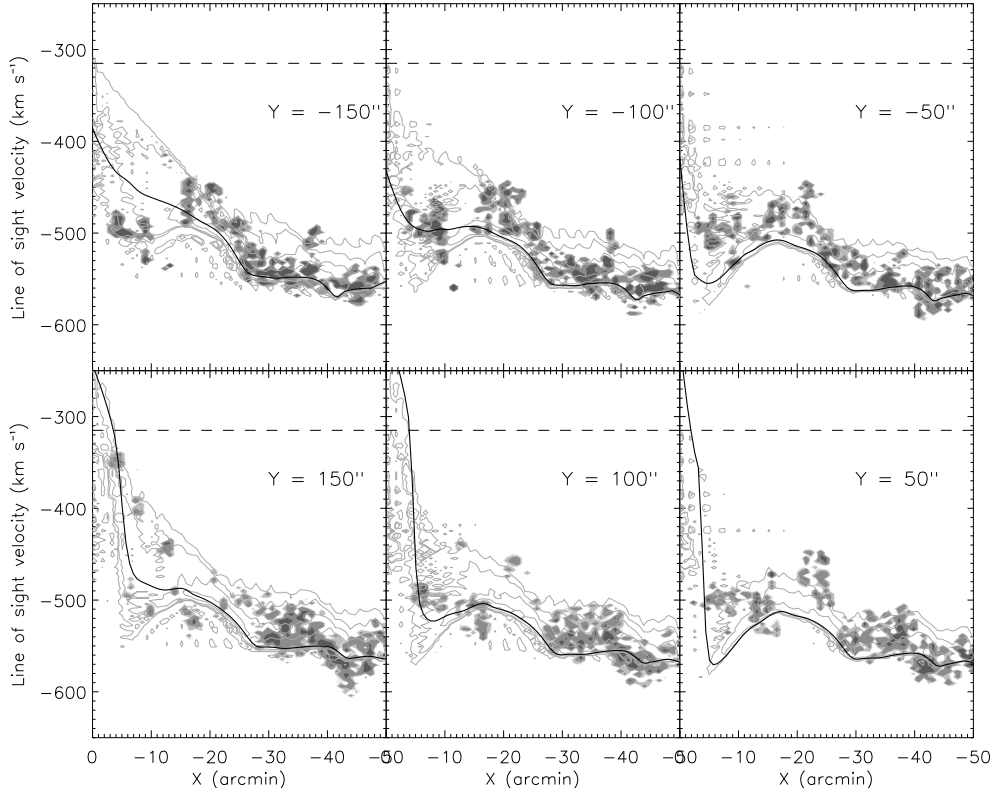


Figure 3. Comparison of CO observations and gas velocities from the model of maximum likelihood away from the line of nodes of the disk. The model includes a thick disk of scale height $z_0 = 200$ pc and a loss of velocity of $0.3 v_0 \text{ kpc}^{-1}$ away from the plane of the disk. Model data were convolved with the 2D function representing the FCRAO beam as described in the text. Intensity is plotted as a greyscale for observations and using contour levels for model data. Contours are given at 1, 3, 10 and 30% of the maximum value in each subplot. The dashed line indicates the systemic velocity and the solid line the results at Y arcsec ignoring the effects of the thick disk and of the beam function.

light ratio $\Upsilon_B = 6.5$. This in turns implies a bulge mass¹ of $M_{\text{bulge}} = 2.3 \times 10^{10} M_\odot$. The disk mass within the radius of the bulge (3.5 kpc) can be estimated by assuming reasonable values for the B -band exponential disk central surface brightness ($I_0 = 21.6 \text{ mag arcsec}^{-2}$, Walterbos & Kennicutt 1988) which when corrected for absorption and inclination using the values of Berman (2001) gives a central surface density of $\Sigma_d = 113 L_\odot \text{ pc}^{-3}$, disk scale length ($R_d = 5.8 \text{ kpc}$, Walterbos & Kennicutt 1988), and a conservative disk mass-to-light ratio of 4. This gives a disk mass of $M_{\text{disk}} = 1.2 \times 10^{10} M_\odot$. The total (bulge + disk + halo) mass inside the same radius can be estimated from the rotation curve as $M_{\text{total}} = 3.7 \times 10^{10} M_\odot$, leaving little room for a dark halo.

The value of $\mathcal{R} = 1.2$ found by Berman (2001) implies that the bulge of M31 is a fast rotator. Interestingly, of the few galaxies for which \mathcal{R} has been measured, all have been found to be fast rotators. Debattista & Sellwood (2000) showed that such fast bars cannot co-exist with massive dark halos because dynamical friction would slow them down rapidly. The value of $\mathcal{R} = 1.2$ is further evidence that M31 must have a minimal halo, and, consequently, a maximum

disk. This is notably at odds with the contentions of Cold Dark Matter (CDM) models, which predict massive halos and minimal disks (e.g. Navarro et al. 1997).

3 MODELLING OFF-AXIS OBSERVATIONS

As mentioned earlier, Berman (2001) pointed out that a much stronger case could be made for his best fit model if it were found to be consistent with observations of CO velocities away from the line of nodes of the disk. Moreover, it is important to utilize these off-axis velocities since dynamical models of the bulge of M31 have never before been constrained by real 3D (X, Y, V) observations.

To compare accurately the output of the model with the data, we performed a 2D convolution of the model with a realistic description of the FCRAO beam, consisting of the sum of a sinc function and two Gaussians. The side-lobes of the sinc function provide a good (very conservative) description of any coma effects, while the two Gaussians describe the response of the FCRAO antenna to emission coming from angles far away from the nominal pointing position, due to the imperfections of the dish (Ladd & Heyer 1996). The sinc function has a full width at half maximum (FWHM) of 45 arcsec and the two Gaussians have FWHM and attenuations of 30 arcmin and 30 dB, and 4 degrees and

¹ The value given for the mass of the bulge in Berman (2001) was not correct. The amended version has been used in this paper.

50 dB, respectively. This convolution produces multiple velocities at each X position in the (X, V) position–velocity diagrams derived from the model, in the same way as multiple velocities arise naturally in the data cube.

Fig. 1 shows position–velocity diagrams for observational data at $Y = \pm y \times 50$ arcsec, where $y = 1, 2, 3$. Overlaid are Berman’s best fit model’s predictions convolved with the FCRAO beam function which should, if the model is correct, approximately enclose the observations on every plot. In this, as in all of the comparisons below, the model has been interpolated to fit the positions of the observations. Although the general trends of the predictions and the observations are similar, the model data enclose a narrower range of velocities than the observations and are further from the systemic velocity than the observations. The discrepancies are just as large or greater for models with different input parameters. In particular, it is not reasonable to use a smaller rotation velocity. This would help reconcile the predictions of the model proposed by Berman (2001) with the data in the central regions, but would predict velocities much too small at distances larger than about 40 arcmin from the centre.

The same ‘beard’ phenomenon is seen in the position–velocity diagrams of the spiral galaxy NGC 2403 (fig. 1 of Schaap et al. 2000). The arguments presented in that paper conclude that the beard is either caused by a thick high density gas layer with a half width at half maximum (HWHM) intensity of 500 pc or a lower density layer with HWHM of 1.75 kpc, rotating more slowly than the standard thin disk. This conclusion is motivated by galactic fountain models (Spitzer 1990) in which hot gas from supernova explosions and galactic winds rises from the disk into the halo. As it rises, the gravitational attraction towards the centre of the galaxy lessens, the gas moves outwards and, by conservation of angular momentum, its azimuthal velocity decreases. Thick molecular disks have been seen in CO in the Milky Way Galaxy (Dame & Thaddeus 1994), and the edge-on spiral galaxy NGC 891 (Garcia-Burillo et al. 1992).

To recover the small magnitude and large range of velocities of the observations of M31, the bulge model of Berman (2001) is augmented by the kinematics of a thick disk which has been rotated and inclined to the observer’s frame. The vertical density distribution follows Schaap et al. (2000) in taking a Gaussian form

$$\rho(z) = \rho_0 \exp(-z^2/2z_0^2), \quad (1)$$

$$\rho_0 = \frac{\Sigma_0}{(2\pi)^{1/2} z_0}, \quad (2)$$

where ρ_0 and Σ_0 are the density and surface density respectively at $z = 0$, and z_0 is the vertical scale height of the gas. The half width at half maximum intensity $z_{1/2} = 1.18 z_0$. The intensities at (X, Y) are convolved in 2D with the function representing the FCRAO beam as described earlier, to produce position–velocity plots for $Y = \pm y \times 50$ arcsec, where $y = 1, 2, 3$. Fig. 2 compares the observational data with the results from a model with $z_0 = 400$ pc, the lowest value of the scale height that adequately encloses the vast majority of the observations for $X > -50$ arcmin. For this model, $z_{1/2} = 472$ pc. This is very large when compared to the thick disk observed by Dame & Thaddeus (1994) in the Milky Way, for which HWHM is between 71 and 133 pc depending on position, but smaller than the thick disk

of NGC 891 (Garcia-Burillo et al. 1992), where HWHM is larger than 1 kpc.

We now follow Schaap (2000) and drop the implicit assumption that the thick disk is corotating with the $z = 0$ plane and reduce the velocities of the gas where $z \neq 0$. Velocities parallel to the z axis stay fixed at zero. A slow thick disk is implied by the galactic fountain models and was also invoked by Swaters et al. (1997) to explain the H I observations of NGC 891. We take the linear velocity distribution used in both papers:

$$\mathbf{v}(z) = \mathbf{v}_0(1 - \gamma z), \quad (3)$$

where \mathbf{v}_0 is the velocity in the $z = 0$ plane, γ is the velocity lost per kpc and z is the height. By slowing the gas down above and below the plane of the disk, the range of velocities at a particular scale height is extended. It can be seen in Fig. 3 that a similar range of velocities to both the observations and the corotating model is produced if the scale height is just 200 pc and $\gamma = 0.3$ i.e. the gas loses 30% of its speed per kpc away from the plane of the disk. This implies that $z_{1/2} = 236$ pc which is closer to but still larger than the values quoted for the Milky Way in Dame & Thaddeus (1994) and much smaller than the value for NGC 891.

By including a thick disk, the model initially proposed by Berman (2001) is able to match the 3D CO data of Loinard et al. (1999) reasonably well. The most noticeable discrepancy is found around $X = \pm 20 - 25$ arcmin, $V \sim -45$ km s $^{-1}$, a position that the original model found difficult to account for even along the line of nodes of the disk. It is plausible that some vertical or turbulent gas motions not included in our model can account for these remaining discrepancies.

As mentioned above, galactic fountain models are often invoked to account for thick gaseous disks in the centres of galaxies. However, they are probably not justifiable in M31 since it does not harbour a great deal of star formation. Moreover, whilst the thick disk found by Dame & Thaddeus (1994) in the Milky Way appears to be much fainter in CO than the Galactic mid–plane, the present modelling requires that in M31 it be just as bright. A plausible alternative follows from the recent work by Martos & Cox (1998), who describe many numerical simulations combining magnetic fields with hydrodynamics to create postshock regions in which large pressure gradients exist near to the mid–plane causing the gas layer to expand vertically. The result is a ‘hydraulic jump’ in which a build up of gas in the vertical direction can be seen with scale heights of hundreds of parsecs.

Another, perhaps more controversial, possibility should be mentioned here. Pringle et al. (2001) contend that much of the ISM in spiral galaxies is molecular, but too cold to be easily detectable in CO. In this view, only the parts of molecular clouds illuminated by newly formed stars are bright in CO. The CO–bright thin disk could then correspond to the thin layer where stars form most actively, whereas the thick disk would correspond to the real total extent of the molecular layer. The existence of large quantities of cold molecular gas in the inner regions of M31 has been proposed by Loinard & Allen (1998 – and references therein). Moreover, since the inner region of M31 harbours little star–forming activity, the thin disk there would not be particularly brighter

6 *Simon Berman and Laurent Loinard*

in CO than the thick disk, and the distinction between the two would indeed vanish.

Finally, a last possibility is that the inner disk of M31 is actually thin, but warped. Modelling it as a thick disk then becomes a convenient way to account for the gas located in the warped parts of the disk, above or below the mid-plane.

4 CONCLUSIONS

In this article, we show that hydrodynamical triaxial models of the bulge of the Andromeda galaxy (M31) previously presented by Berman (2001), and initially tested against CO emission observations along the apparent major axis only, can also account for the CO emission velocities observed off the apparent major axis – a much more robust validity test. The triaxial model implies that the bulge of M31 is a fast rotator and hence the dark matter contained in its central regions must be minimal and coincident with the stellar disk.

To account for the whole velocity range covered by the observations, a finite, fairly large thickness (half width at half maximum intensity of 200–500 pc) must be given to the molecular disk. It is quite unclear, however, whether the inner molecular disk of M31 is truly that thick or whether adding it to the model is merely an effective theoretical trick able to account for a warping of a thinner disk. Other out of plane, or peculiar velocities (such as those associated with hydraulic jumps or turbulence) could also contribute to the wide velocity range covered by the CO observations.

ACKNOWLEDGMENTS

We thank James Binney and Daniel Pfenniger for careful reading of the manuscript, and interesting comments.

REFERENCES

Berman S., 2001, *A&A*, 371, 476
Binney J. J., Gerhard O. E., Spergel D., 1997, *MNRAS*, 288, 365
Brinks E., Burton W.B., 1984, *A&A*, 141, 195
Brinks E., Shane W.W., 1984, *A&AS*, 55, 179
Martos M. A., Cox D. P., 1998, *ApJ*, 509, 713
Dame T. M., Thaddeus P., 1994, *ApJ*, 436, L173
Dame T. M., Koper E., Israel F. P., Thaddeus P., 1993, *ApJ*, 418, 730
Dame T. M., Hartmann D., Thaddeus P., 2001, *ApJ*, 547, 792
Debattista V. P., Sellwood J. A., 2000, *ApJ*, 543, 704
Dwek, E. et al. 1995, *ApJ*, 445, 716
Garcia-Burillo S., Guélin M., Cernicharo J., Dahlem M., 1992, *A&A*, 266, 21
Gerhard O. E., Vietri M., 1986, *MNRAS*, 223, 377
Kerr F. J., 1967, *IAUS*, 31, 239
Ladd N., Heyer, M. H., 1996, FCRAO technical memorandum
Lindblad B., 1956, *Stockholms Observatoriums Annaler*, 2
Loinard L., Allen R. J., 1998, *ApJ*, 499, 227.
Loinard L., Allen R. J., Lequeux J., 1995, *A&A*, 301, 68.
Loinard L., Dame T. M., Koper E., Lequeux J., Thaddeus P., Young J. S., 1996, *ApJ*, 469, L101
Loinard L., Dame T. M., Heyer M. H., Lequeux J., Thaddeus P., 1999, *A&A*, 351, 1087
Mulder W. A., Liem B. T., 1986, *A&A*, 157, 148
Navarro J. F., Frenk C. S., White S. D. M., 1997, *ApJ*, 490, 493
Pringle J. E., Allen R. J., Lubow S. H., 2001, *MNRAS*, 327, 663
Rougoor G. W., Oort J. H., 1959, *IAUS*, 9, 416
Schaap W. E., Sancisi R., Swaters R. A., 2000, *A&A*, 356, 49
Spitzer L. Jr., 1990, *ARA&A*, 28, 71
Stark A. A., 1977, *ApJ*, 213, 368
Stark A. A., Binney J., 1994, *ApJ*, 426, 31
van Albada G. D., van Leer B., Roberts W. W., 1981, *ApJ*, 108, 76
Walterbos R. A. M., Kennicutt R. C., 1988, *A&A*, 198, 61